Inter-DNA Attraction Mediated by Divalent Counterions

Xiangyun Qiu, Kurt Andresen, Lisa W. Kwok, Jessica S. Lamb, Hye Yoon Park, and Lois Pollack
School of Applied and Engineering Physics, Cornell University, Ithaca, New York 14853, USA
(Received 2 March 2007; published 20 July 2007)

Can nonspecifically bound divalent counterions induce attraction between DNA strands? Here, we present experimental evidence demonstrating attraction between short DNA strands mediated by Mg^{2+} ions. Solution small angle x-ray scattering data collected as a function of DNA concentration enable model independent extraction of the second virial coefficient. As the $[Mg^{2+}]$ increases, this coefficient turns from positive to negative reflecting the transition from repulsive to attractive inter-DNA interaction. This surprising observation is corroborated by independent light scattering experiments. The dependence of the observed attraction on experimental parameters including DNA length provides valuable clues to its origin.

DOI: 10.1103/PhysRevLett.99.038104 PACS numbers: 87.14.Gg, 87.15.Nn, 87.64.Bx

Electrostatic interactions are fundamental to the complex structure and dynamics of nucleic acids due to their highly charged nature. Positively charged ions counteract and can even reverse the repulsion between negatively charged nucleic acids [1,2]. Quantitative studies of counterion mediated interactions are essential in understanding phenomena such as DNA condensation and packaging [1,2] and RNA folding [3].

Counterion valence is a critical factor in modulating inter-DNA forces. In the presence of monovalent cations (e.g., Na^+), the dominant force between DNA strands is like charge repulsion. Following the seminal Derjaguin, Landau, Verwey, and Overbeek (DLVO) mean field theory [4], this interaction can be described by a Yukawa pair potential. To correct for the linear Poisson-Boltzmann approximation in the DLVO theory, the charge renormalization prescription [5] assigns an effective charge Z_{eff} to each DNA. The Yukawa form of the repulsive inter-DNA potential has been validated by our recent measurements, though the measured effective charges are smaller than predicted [6]. In the presence of low concentrations of counterions of tri- or higher valence, strong attractive forces between DNA strands (e.g., precipitation) are observed [1,2]. The phase diagram of such ''precipitated'' liquid crystalline DNA complexes has been studied in detail [7]. However, the exact physical origin of the like charge attraction remains elusive [8]. Proposed competing mechanisms for attraction include counterion local density fluctuations [9,10], positional correlation between condensed counterions [11,12], and tight binding of counterions along discrete charged DNA monomers [13–15]. Notably, strong electrostatic coupling may lead to overcharging due to counterion ''Wigner-lattice'' [16] or Bjerrum pairing correlations [17].

The ability of nonspecifically bound divalent counterions (e.g., Mg^{2+}) to induce attractive interaction between DNA strands remains controversial. Both analytical theories and simulations have predicted net short range attractive forces between DNA strands in divalent (2:1) salts [11,13,18,19]. Experimental support for the predicted attractions remains tentative. Our previous measurement of the inter-DNA forces in the presence of divalent ions suggested a weak attractive interaction under $[Mg^{2+}] > 16$ mM [6], though this conclusion was based on the assumption of a particular model calculation. It should also be noted that inter-DNA attraction has been proposed even in monovalent salts based on observations of the ''slow mode'' in dynamic light scattering and low angle ''upturns'' from small angle neutron scattering [20]. Notably, condensation of DNA by divalent Mg^{2+} counterions has never been observed in bulk solution [21]. By monitoring the conformational changes of a tethered DNA system [22], Bai *et al.* rule out possible strong inter-DNA attraction up to 600 mM Mg^{2+}, which is also consistent with the lack of discontinuity in inter-DNA spacings upon increasing osmotic stress [23]. Here, we aim to establish beyond doubt the existence of inter-DNA attraction mediated by divalent counterions.

Small angle x-ray scattering (SAXS) measurements of semidilute double strand DNA (dsDNA) solutions were carried out at the C1 and G1 stations of the Cornell High Energy Synchrotron Source (CHESS). The x-ray exposure time was chosen to ensure time-independent scattering profiles. Single strand DNA oligomers were purchased from Integrated DNA Technologies and annealed at pH 7.5 to obtain rigid rodlike dsDNA (8, 16, and 25 base pairs). Each sample was dialyzed against monovalent (NaCl) or divalent ($MgCl_2$) salt solutions buffered with 1 mM pH = 7 NaMOPS [sodium 3-(N-morpholino)propanesulfonic acid]. Neither Na^+ nor Mg^{2+} displays site-specific binding to DNA [24]. The measured scattering intensity $I(Q)$ [$Q = (4\pi/\lambda)\sin\theta$, λ is the x-ray wavelength, and 2θ is the scattering angle] has two components: the form factor $P(Q)$ of a single DNA and the structure factor $S(Q)$. The inter-DNA interference function $S(Q)$ arises from long range structural correlations, modulates the SAXS profile, and is most pronounced at low Q [25].

Qualitatively, inter-DNA repulsion causes a decrease or downturn in $I(Q)$ at the lowest Q and possibly a finite Q peak if sufficiently strong. In contrast, attraction results in a low Q increase or upturn due to molecular clustering. However, extraction of $S(Q)$ from experimental data requires knowledge of the form factor $P(Q)$, which is nontrivial to predict even when the atomic coordinates of the DNA are known [25]. We can avoid this complication by collecting SAXS profiles under identical ionic conditions [i.e., identical $P(Q)$'s], while varying DNA concentrations alone. The nature of inter-DNA force can then be conclusively assessed *solely by experiments* by the appearance of a low Q downturn (repulsion) or upturn (attraction) in the [DNA] normalized SAXS profiles upon increasing [DNA]. Such experimental data are shown in Fig. 1 and indicate that the inter-DNA force varies from repulsive at $[Mg^{2+}]$ of 3 mM to marginally repulsive at $[Mg^{2+}]$ of 10 mM. The opposite trends at $[Mg^{2+}]$ of 50 and 200 mM present clear evidence for inter-DNA attraction.

Is the observed inter-DNA attraction solely due to divalent Mg^{2+} ions? Other factors such as coions and reduced solvent activity in concentrated salts merit careful consideration. To control for these effects, we replaced Mg^{2+} with monovalent Na^{+} ions with the same coion Cl^{-} and ionic strengths and measured similar DNA concentration series. Figure 2 shows that the inter-DNA repulsion is much stronger in NaCl of the same ionic strength. Even 150 mM NaCl can not fully screen the electrostatic repulsion. This repulsion nearly vanishes only at [NaCl] above 600 mM. Importantly, no inter-DNA attraction is observed with even higher monovalent salt concentrations. Thus, Mg^{2+} ions induce the inter-DNA attraction.

The near perfect rigidity of short dsDNA strands (e.g., ~80 Å for 25 bp DNA) eliminates the intra-DNA degrees of freedom, enabling reliable quantitative analysis of inter-DNA interactions. However, most theories consider charged cylinders to have infinite length. Whether this assumption breaks down is contingent on two length scales: the DNA length and the Debye screening length. When they become comparable, so-called "end effects" can become significant [26]. Therefore, by varying DNA length only, while maintaining similar total phosphate concentrations and the same Debye screening length (17 Å at $[Mg^{2+}]$ of 10 mM), we probed the length dependence of the inter-DNA forces. Figures 2(e) and 2(f) show low Q upturns (i.e., attraction) upon increasing [DNA] for 16 bp (54 Å long) and 8 bp (27 Å long) dsDNA strands, respectively. Given that the 25 bp dsDNA still shows marginal repulsion at $[Mg^{2+}]$ of 10 mM [Fig. 1(b)], this suggests that shorter DNA results in stronger attraction (discussed later).

For a model independent analysis, enabling quantitative comparisons between different DNA and ionic conditions, we turn to a well-established assay of interparticle interactions: computing the second virial coefficients from SAXS profiles. The second virial coefficient is derived from the following equation,

$$\frac{P(Q=0)}{I(c,Q=0)} = \frac{1}{S(c,Q=0)} = 1 + (2MA_2)c, \qquad (1)$$

where c is the [DNA] in g/ml, M is the molecular weight, and A_2 is the second virial coefficient. The $I(c, Q = 0)$ is extrapolated by fitting the Guinier region of experimental $I(Q)$ [27]. Thus, A_2 can be obtained through linear fitting, noting that the $P(Q = 0)$ is also fitted. Excellent linearities of $1/S(c, Q = 0)$ are evident in Figs. 3(a)–3(c). Here a positive slope indicates repulsion, while a negative one indicates attraction. Figure 3(a) demonstrates the presence of inter-DNA repulsion only under monovalent counter-

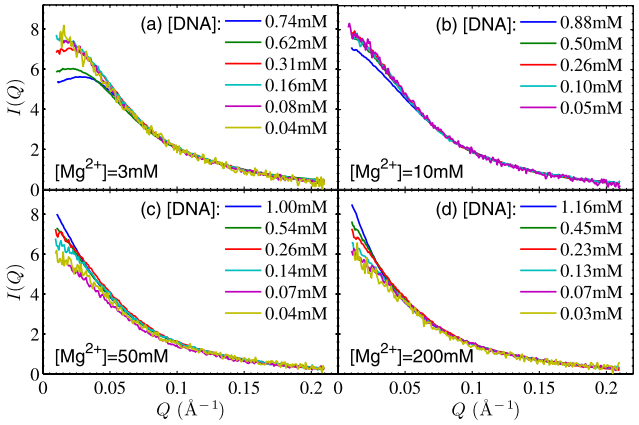

FIG. 1 (color online). Experimental $I(Q)$'s from 25 bp DNA strands as a function of [DNA] are shown in each panel at a given $[Mg^{2+}]$. Each curve has been normalized by [DNA] to enable direct comparisons. The appearance of either a downturn (a),(b) or upturn (c),(d) at the lowest scattering angle indicates repulsion or attraction between DNA strands.

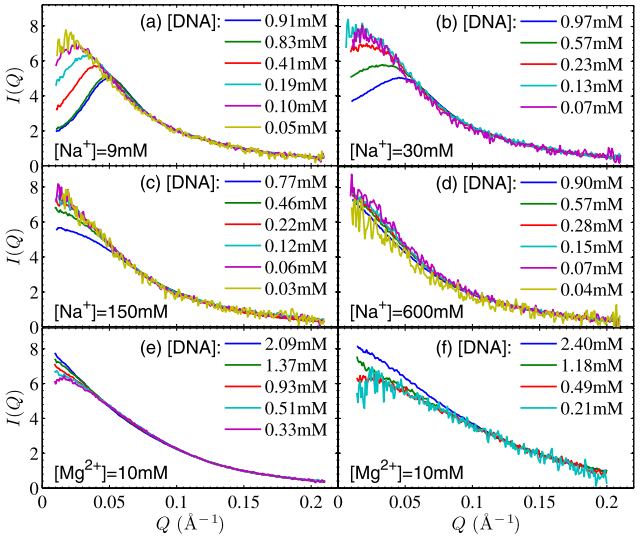

FIG. 2 (color online). As in Fig. 1, experimental $I(Q)$'s as a function of [DNA] are shown in each panel for 25 bp (a)–(d), 16 bp (e), and 8 bp (f) DNA strands. No attraction is observed at any measured $[Na^{+}]$ for 25 bp DNA, while weak attraction is indicated for 16 bp and 8 bp DNA strands at $[Mg^{2+}]$ of 10 mM.

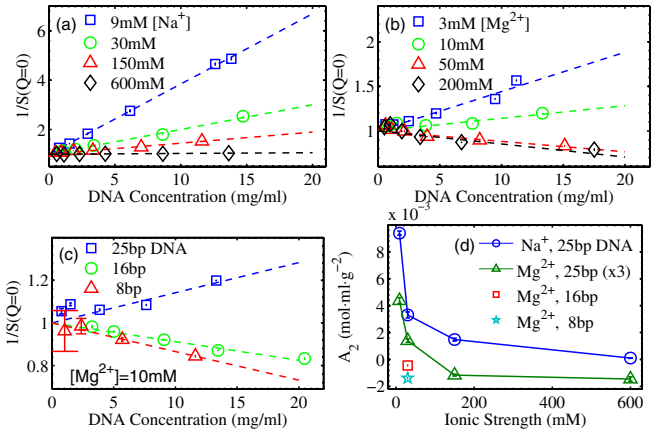

FIG. 3 (color online). Interactions between DNA strands are reflected by changes in the y intercept of $I(Q)$ [$\propto S(c, Q = 0)$]. Here $1/S(c, Q = 0)$ (symbols) is shown as a function of [DNA] (a) at different [Na^+], (b) at different [Mg^{2+}], and (c) as a function of DNA length at 10 mM Mg^{2+}. The second virial coefficient can be derived from these data according to Eq. (1). The variation of A_2 as a function of ionic strength is shown in (d). Both repulsion ($A_2 > 0$) and attraction ($A_2 < 0$) are observed as [Mg^{2+}] increases; however, only repulsion is observed in the presence of monovalent ions. The data for 25 bp DNA in Mg^{2+} are multiplied by a factor of 3 for clarity. Most error bars have sizes comparable to symbols.

ions, while Fig. 3(b) shows the crossover from repulsion to attraction upon increasing [Mg^{2+}]. The comparison of DNA strands of different lengths [Fig. 3(c)] confirms stronger attraction (i.e., larger negative slope) with shorter DNA strands. Figure 3(d) compares the second virial coefficient A_2 as a function of ionic strength for all DNA lengths and counterion types. This chart makes it possible to find equivalent salt conditions giving the same inter-DNA interaction, e.g., 150 mM $Na^+ \approx 3$ mM Mg^{2+}.

To further substantiate the observed inter-DNA attraction from SAXS experiments, we carried out independent light scattering measurements of the second virial coefficients. Selected 25 bp DNA samples were prepared following the same protocol and were measured with the dynamic light scattering instrument Malvin Zetasizer Nano Series (Laser 4 mW He-Ne, 633 nm). At each salt condition, a series of samples with different DNA concentrations was measured at 25 °C. All solutions were filtered twice to eliminate dust. The measured A_2 values at [Mg^{2+}] of 3, 5, and 200 mM are $2.2e$–3, $-6.8e$–4, and $-1.1e$–3 mol ml g^{-2}, respectively. The values not only qualitatively confirm the nature of attractive interaction at 50 and 200 mM Mg^{2+}, but also show reasonable quantitative agreement with SAXS measurements. We also measured at conditions of 10 mM $pH = 7$ NaMOPS and/or 0.1 mM $pH = 7$ ethylenediamine tetraacetic acid (EDTA) to check for possible pH dependence and high valence metal ion contamination. No detectable change was observed with the addition of 0.1 mM EDTA, while only a slight decrease of inter-DNA attraction (A_2 from $-6.8e$–4 to $-6.3e$–4 mol ml g^{-2}) results from the 1 to 10 mM increase in NaMOPS concentration at [Mg^{2+}] of 50 mM, presumably due to the effect of counterion competition. Possible multivalent ion contamination or pH effects are thus eliminated.

In addition to second virial coefficients, detailed information on inter-DNA potentials can be obtained by quantitatively analyzing the *full SAXS profiles*. As in our recent study [6], the generalized one-component method (GOCM) [28,29] is used to compute the structure factor $S(Q)$ from a model Yukawa pair potential with a hard core repulsion (as in DLVO theory). Instead of measuring the form factor at each condition, we *numerically* compute the $P(Q)$'s from known DNA structure, accounting for solvent effects such as hydration and "condensed" counterions. Comparisons with available measured form factors show reasonable agreement. In the refinement of the full SAXS profile, the only free parameter is the effective charge Z_{eff} in the Yukawa potential. A more detailed description of analysis methods can be found in Ref. [6]. Although the mean spherical approximation (MSA) holds only in the dilute DNA limit, application of MSA allows for convenient quantitative analysis, and is supported by the agreement between predictions and experimental data in the semidilute DNA regime.

Figure 4(a) shows the SAXS profiles as a function of [Mg^{2+}] at [DNA] ~0.7 mM. The fitted structure factor $S(Q)$'s shown in Fig. 4(b) demonstrate the transition from repulsion (low Q downturn) to attraction (low Q upturn) upon increasing [Mg^{2+}]. The measured effective charges (Z_{eff}) are 13.23, 7.14, 4.50, 2.89, and 0.71 elemental charge with [Mg^{2+}] of 0, 1, 2, 3, and 4 mM, respectively. This is in drastic contrast with the measured $Z_{\text{eff}} \sim 12e$ with monovalent Na^+ ions which only weakly depends on ionic strength [6]. At [Mg^{2+}] of 10 mM, the interaction between DNA strands vanishes as the structure factor approaches unity. While the much higher screening efficiency of Mg^{2+} versus Na^+ is not surprising [30], inter-DNA attraction, i.e., the low Q upturn, is observed when [Mg^{2+}] > 10 mM, and increases with [Mg^{2+}]. Addition of a second Yukawa potential of short range in the GOCM is able to model the observed attraction [6].

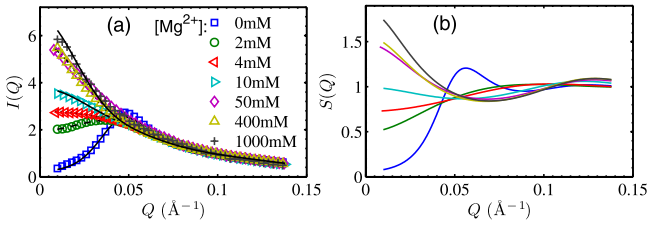

FIG. 4 (color online). The structure factor $S(Q)$ can be extracted from the measured $I(Q)$ using models (see text). Panel (a) shows measured $I(Q)$'s of 25 bp DNA (~ 0.7 mM) (symbols) and the fits (lines). Panel (b) shows the corresponding $S(Q)$'s only with the same color annotation as in (a).

Our experimental results demonstrate conclusively the existence of inter-DNA attraction in divalent Mg^{2+} salts. However, the observed inter-DNA attraction is too weak to induce spontaneous aggregation; e.g., the magnitude of measured A_2 is just in the range of crystallization (not precipitation) conditions of common proteins such as lysozyme [27]. We also independently confirmed the purely electrostatic nature of the interaction between DNA and Mg^{2+} ions by studying ion specific effects of series of divalent ions with similar hydration radii (Mg^{2+}, Ca^{2+}, Sr^{2+}, Ba^{2+}, and Mn^{2+}) at identical free concentrations of 3 mM. While Mn^{2+} and Ca^{2+} ions show much higher screening efficiency, presumably due to specific ion-DNA interactions [24], the same effective charge Z_{eff} ($\sim 2.89e$) of the 25 bp DNA is obtained with Mg^{2+}, Sr^{2+}, and Ba^{2+} ions, indicating pure electrostatic interactions.

The crucial importance of counterion valence (i.e., Mg^{2+} versus Na^{+}) to inter-DNA attraction appears to support the strong electrostatic coupling that forms the basis of counterion correlation and/or tightly bonded ions models [11,13]. For short DNA strands, ''end effects'' are expected to weaken electrostatic coupling [26], thus should result in weaker attraction. In contrast, we observed stronger attraction between shorter DNA strands under the same ionic condition (e.g., 10 mM Mg^{2+}). Here we discuss some potential mechanisms for this unexpected result. First, due to DNA's anisotropic rod shape, the excluded volume (or steric repulsion) decreases faster than linearly with DNA length. The stronger attraction observed may simply be the result of a reduction in repulsion. Interestingly, the measured upturns are well reproduced by calculations of scattering profiles consisting of DNA monomers and dimers formed by direct end-to-end stacking. This suggests that DNA strands may prefer to lie end to end, whereas aforementioned models all predict the strongest attraction when DNA strands lie side by side. We note that end-to-end stacking of short DNA duplexes has been reported in many types of DNA junction structures with the addition of finite concentration of salt [31]. Such an end-to-end attraction may result from base stacking interactions, or possibly from dynamically induced dipolar correlations along the easy polarization axis of DNA strands. In this picture, enhanced attraction for shorter DNA strands might result from the presence of more ''ends'' at a given phosphate concentration. Importantly, attraction is never observed in the presence of Na^{+} ions, thus divalent Mg^{2+} ions clearly play a critical role. This seems to coincide with the requirement of larger counterion valence than DNA monomer charge proposed by de la Cruz *et al.* [15].

In conclusion, we have shown that nonspecifically bound divalent ions (Mg^{2+}) can mediate attractive inter-DNA forces. A series of experiments were carried out to demonstrate the key role of counterion valence. The increase in attraction with decreasing DNA length runs counter to expectation and exemplifies the challenging complexity underlying competing degrees of freedom.

We thank K. Finkelstein, A. Woll, and P. Busch for experimental assistance, the Doniach and Herschlag groups for comments and discussions, Y. Liu and S.-H. Chen for providing their MATLAB codes, and P. Bevilacqua for useful discussion. This research is funded by NIH, NSF, the NBTC at Cornell, and NASA. CHESS is supported by NSF and NIH/NIGMS.

[1] W. Gelbart, R. Bruinsma, P. Pincus, and V. Parsegian, Phys. Today **53**, No. 9, 38 (2000); F. Solis and M. O. de la Cruz, Phys. Today **54**, No. 1, 71 (2001).
[2] V. A. Bloomfield, Biopolymers **44**, 269 (1997).
[3] R. Russell *et al.*, Proc. Natl. Acad. Sci. U.S.A. **99**, 4266 (2002).
[4] E. J. W. Verwey and J. T. G. Overbeek, *Theory of the Stability of Lyophobic Colloids* (Elsevier, New York, 1948).
[5] S. Alexander *et al.*, J. Chem. Phys. **80**, 5776 (1984); P. Gonzalez-mozuelos and M. O. de la Cruz, J. Chem. Phys. **103**, 3145 (1995).
[6] X. Qiu *et al.*, Phys. Rev. Lett. **96**, 138101 (2006).
[7] Y. Burak, G. Ariel, and D. Andelman, Biophys. J. **85**, 2100 (2003); E. Raspaud, D. Durand, and F. Livolant, Biophys. J. **88**, 392 (2005).
[8] G. Wong, Curr. Opin. Colloid Interface Sci. **11**, 310 (2006).
[9] F. Oosawa, Biopolymers **6**, 1633 (1968).
[10] R. Kjellander and S. Marcelja, Chem. Phys. Lett. **112**, 49 (1984).
[11] B. Shklovskii, Phys. Rev. Lett. **82**, 3268 (1999).
[12] I. Rouzina *et al.*, J. Phys. Chem. **100**, 4305 (1996).
[13] Z. Tan and S. Chen, Biophys. J. **91**, 518 (2006).
[14] A. Kornyshev and S. Leikin, Phys. Rev. Lett. **82**, 4138 (1999).
[15] M. O. de la Cruz *et al.*, J. Chem. Phys. **103**, 5781 (1995).
[16] A. Y. Grosberg *et al.*, Rev. Mod. Phys. **74**, 329 (2002).
[17] A. Travesset *et al.*, Europhys. Lett. **74**, 181 (2006).
[18] E. Allahyarov, G. Gompper, and H. Lowen, Phys. Rev. E **69**, 041904 (2004).
[19] N. Gronbech-Jensen, R. J. Mashl, R. F. Bruinsma, and W. M. Gelbart, Phys. Rev. Lett. **78**, 2477 (1997).
[20] R. Borsali *et al.*, Macromolecules **31**, 1548 (1998).
[21] I. Koltover, K. Wagner, and C. R. Safinya, Proc. Natl. Acad. Sci. U.S.A. **97**, 14 046 (2000).
[22] Y. Bai, R. Das, I. S. Millett, D. Herschlag, and S. Doniach, Proc. Natl. Acad. Sci. U.S.A. **102**, 1035 (2005).
[23] D. Rau, B. Lee, and V. Parsegian, Proc. Natl. Acad. Sci. U.S.A. **81**, 2621 (1984).
[24] J. Duguid *et al.*, Biophys. J. **65**, 1916 (1993).
[25] L. Wang and V. Bloomfield, Macromolecules **24**, 5791 (1991); M. Koch, P. Vachette, and D. Svergun, Q. Rev. Biophys. **36**, 147 (2003).
[26] H. J. Limbach and C. Holm, J. Chem. Phys. **114**, 9674 (2001).
[27] F. Bonnete *et al.*, J. Cryst. Growth **196**, 403 (1999).
[28] J. B. Hayter and J. Penfold, Mol. Phys. **42**, 109 (1981).
[29] S. H. Chen *et al.*, J. Appl. Crystallogr. **21**, 751 (1988).
[30] M. L. Henle, C. D. Santangelo, D. M. Patel, and P. A. Pincus, Europhys. Lett. **66**, 284 (2004).
[31] J. Liu *et al.*, J. Mol. Biol. **343**, 851 (2004).